

Directed Motion of Liquid Crystal Skyrmions With Oscillating Fields

A. Duzgun, C. Nisoli, C. J. O. Reichhardt, and C. Reichhardt

Theoretical Division and Center for Nonlinear Studies, Los Alamos National Laboratory, Los Alamos, New Mexico 87545, USA

E-mail: cjrx@lanl.gov

Abstract. Using continuum simulations, we show that under a sinusoidal electric field, liquid crystal skyrmions undergo periodic shape oscillations which produce controlled directed motion. The speed of the skyrmion is non-monotonic in the frequency of the applied field, and exhibits multiple reversals of the motion as a function of changing frequency. We map out the dynamical regime diagram of the forward and reverse motion for two superimposed ac driving frequencies, and show that the reversals and directed motion can occur even when only a single ac driving frequency is present. Using pulsed ac driving, we demonstrate that the motion arises due to an asymmetry in the relaxation times of the skyrmion shape. We discuss the connection between our results and ratchet effects observed in systems without asymmetric substrates.

1. Introduction

Skyrmions are particle like textures that arise in chiral magnets [1, 2, 3, 4] and chiral liquid crystal systems [5, 6, 7, 8, 9, 10, 11]. When either confinement or strong electric fields are present, the liquid crystal (LC) system can form a uniform nematic, a cholesteric stripe, or a meron lattice. Recently, experiments on LC skyrmions or baby skyrmions revealed directional motion in which the skyrmion translates in one direction under an oscillating applied electric field. The motion appears when there is a combination of two different modulation frequencies of the electric field which generate rotation in and out of the plane of the director field on one side of the skyrmions [9, 10]. Similar directed motion was also observed in two-dimensional continuum simulations [9]. In theoretical studies using coarse-grained models in which the skyrmions are represented as solitons, directed motion emerges when the skyrmions move in a direction perpendicular to the tilt of the background director, but are unable to move as rapidly in the opposite direction when the field is removed [12].

Skyrmions in chiral magnets also undergo directed motion under an oscillating field, and by superimposing multiple driving fields, it is possible to achieve controlled steering of the skyrmions [13, 14, 15, 16, 17]. The directed motion in this case arises due to asymmetry in the oscillations of the skyrmion shape, and can be described in terms of a ratchet effect [18]. Ratchet effects also arise for the ac driving of skyrmions coupled to an asymmetric substrate [19, 20, 21, 22, 23]. For liquid crystal skyrmions, open questions include what ac driving protocols can be used to produce directed motion, such as whether a single ac driving frequency is sufficient to produce such motion, and whether reversals between forward and backward motion or even multiple reversals occur as the driving parameters are varied. It is also interesting to explore whether ac drives that are not sinusoidal can produce controlled directed motion.

In this work we examine the ratchet-like motion of a liquid crystal skyrmion under an oscillating ac field with either a single driving frequency or multiple superimposed driving frequencies. We show that the skyrmion can translate in either the forward or backward direction, and that multiple reversals of the motion can occur as the driving frequency is varied. We map out the different directed motion regimes for multiple frequency driving, and show that it is possible to induce motion in each direction using only a single ac driving frequency. The directed motion and reversals also appear when we replace the sinusoidal driving by periodic square wave pulses, which reveal more clearly that the directed motion results from different modes of skyrmion motion during different portions of the driving cycle. We discuss the relevance of our results to other ratchet systems in which directed motion can occur in the absence of an asymmetric substrate.

2. Numerical Methods

We consider a single liquid crystal skyrmion under two oscillating fields using continuum based simulations of the type employed previously to model LC skyrmions [10, 24, 25]. In the continuum description, the traceless tensor Q relates the scalar order parameter S to the orientational order of a chiral nematic liquid crystal state, which under proper constraints will support skyrmions in systems confined between two substrates with normal surface anchoring. The free energy density has the form

$$f = \frac{a}{2} \text{Tr}(Q^2) + \frac{b}{3} \text{Tr}(Q^3) + \frac{c}{4} [\text{Tr}(Q^2)]^2$$

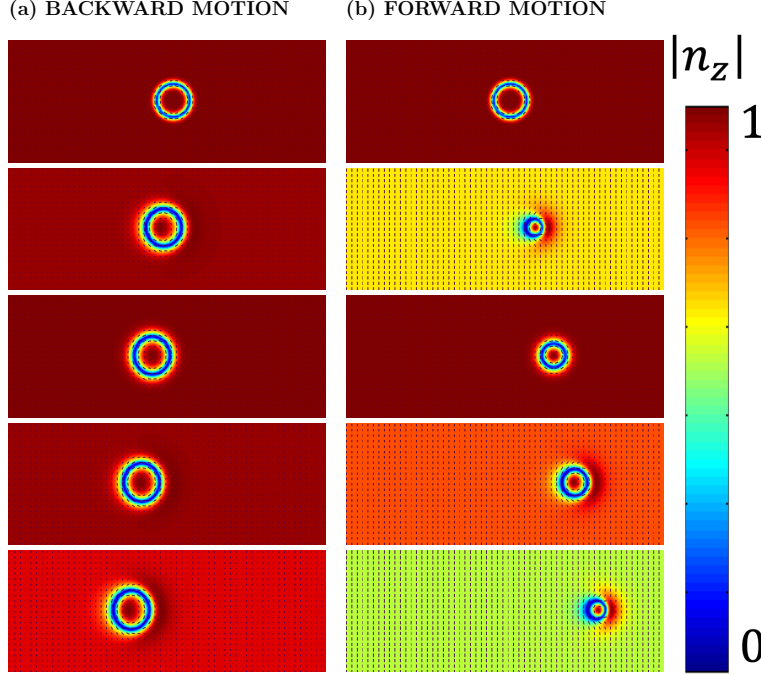


Figure 1. The skyrmion positions and motion over time under ac driving. Color indicates the magnitude of the director field $|n_z|$ in the z direction, and time increases from top to bottom. (a) $A = 0.1$, where the skyrmion translates in the negative x -direction with $2\pi/\omega_1 = 1.2 \times 10^3$ and $2\pi/\omega_2 = 1 \times 10^4$. (b) $A = 0.2$, where the skyrmion moves in the positive x -direction with $2\pi/\omega_1 = 1.2 \times 10^5$ and $2\pi/\omega_2 = 1 \times 10^6$.

$$\begin{aligned}
 & + \frac{L}{2} (\partial_\gamma Q_{\alpha\beta}) (\partial_\gamma Q_{\alpha\beta}) - \frac{4\pi}{p} L \epsilon_{\alpha\beta\gamma} Q_{\alpha\rho} \partial_\gamma Q_{\beta\rho} \\
 & - K [\delta(z) + \delta(z - N_z)] Q_{zz} - \Delta\epsilon E^2 \hat{\mathbf{n}} \cdot \mathbf{Q} \cdot \hat{\mathbf{n}} , \quad (1)
 \end{aligned}$$

where the nematic to isotropic transition is controlled by the terms $(a/2) \text{Tr}(Q^2) + (b/3) \text{Tr}(Q^3) + (c/4) [\text{Tr}(Q^2)]^2$, and the elastic energies with respect to a gradient in Q , using the single elastic constant approximation, are $(L/2) (\delta_\gamma Q_{\alpha\beta}) (\partial_\gamma Q_{\alpha\beta}) - (4\pi/p) L \epsilon_{\alpha\beta\gamma} Q_{\alpha\rho} \partial_\gamma Q_{\beta\rho}$, which favor a twist with cholesteric pitch p . The homeotropic surface anchoring from the boundaries and the electric field of magnitude E along the unit vector $\hat{\mathbf{n}}$ arise in the last line with a coupling strength K and dielectric anisotropy $\Delta\epsilon$. On the surfaces, the Q tensor has uniaxial perfect ordering in the z direction. The electric field E arises due to a potential difference across the slab. The skyrmion dynamics are obtained from the following overdamped equation: $\partial_t Q(\mathbf{r}, t) = -\Gamma \delta F / \delta Q(\mathbf{r}, t)$, where $F = \int f(\mathbf{r}) d^3r$ and Γ is the mobility constant. As in previous work [10, 24, 25] we employ z -invariant (2D) skyrmions [26]. The out of plane rotation of skyrmions is generated by tilting the background electric field. This ac driving is produced by an E field $\mathbf{E} = E[\sin(\theta)\hat{\mathbf{y}} + \cos(\theta)\hat{\mathbf{z}}]$ which is periodically switched between the positive z direction and the positive y direction, with polar angle $\theta = (\pi/6)[\cos(\omega_1 t) \cos(\omega_2 t)]^2$.

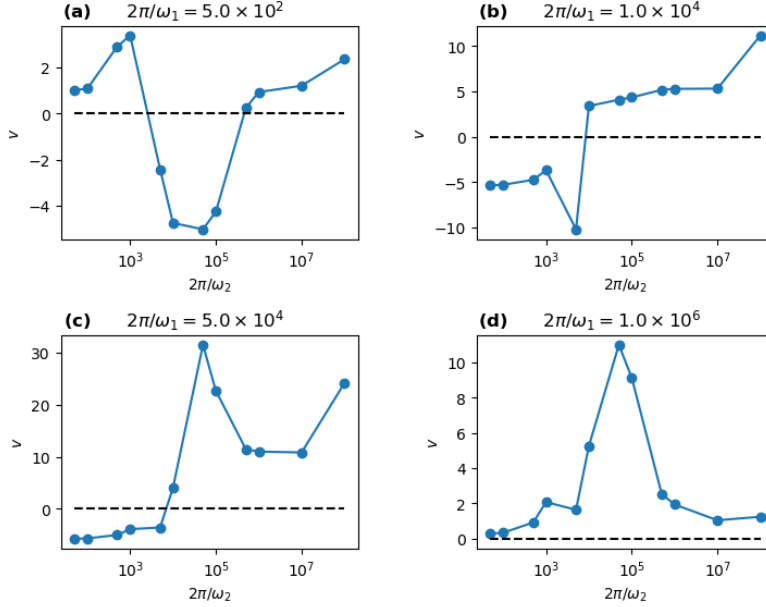


Figure 2. The skyrmion velocity v versus $2\pi/\omega_2$ for the system in Fig. 1 at $2\pi/\omega_1 =$ (a) 5×10^2 , (b) 1×10^4 , (c) 5×10^4 , and (d) 1×10^6 . There can be multiple reversals in the direction of motion as a function of frequency.

3. Results

In Fig. 1 we show an image of the skyrmion under ac driving, where the color code indicates the magnitude of the director field $|n_z|$ in the z direction. In this case, when the electric field is tilted toward the positive y axis, the background director field is also tilted toward y but the skyrmion shape is deformed along the x direction such that a crescent shape region of vertical directors form on the positive x side of the skyrmion. Here the electric field is oscillated between the z direction and the positive y direction. The skyrmion translates in the negative x or backward direction in Fig. 1(a), where the parameters of the ac drive are $2\pi/\omega_1 = 1.2 \times 10^3$ and $2\pi/\omega_2 = 1 \times 10^4$, while in Fig. 1(b), the same skyrmion under ac driving with $2\pi/\omega_1 = 1.2 \times 10^5$ and $2\pi/\omega_2 = 1 \times 10^6$ moves in the positive x or forward direction. Crucially, in each case, an asymmetry in the skyrmion shape appears in the orientation of the director field.

We next hold ω_1 fixed while varying ω_2 , and measure the skyrmion velocity over a fixed number of ac drive cycles. In Fig. 2(a) we plot the skyrmion velocity v versus $2\pi/\omega_2$ for a system with fixed $2\pi/\omega_1 = 5 \times 10^2$. For low frequencies, the skyrmion translates in the positive x direction, but there a reversal to motion in the negative x direction for $1 \times 10^3 < 2\pi/\omega_2 < 1 \times 10^5$, followed by a second reversal to positive x direction motion for $2\pi/\omega_2 > 1 \times 10^5$. The magnitude of the maximum velocity in the $-x$ direction is more than two times larger than the magnitude of the maximum velocity in the $-y$ direction.

In Fig. 2(b) we plot the skyrmion velocity for a sample with a much higher fixed frequency of $2\pi/\omega_1 = 1 \times 10^4$. For low values of $2\pi/\omega_2$, the skyrmion moves in the negative x direction, while a transition to motion in the positive x direction appears

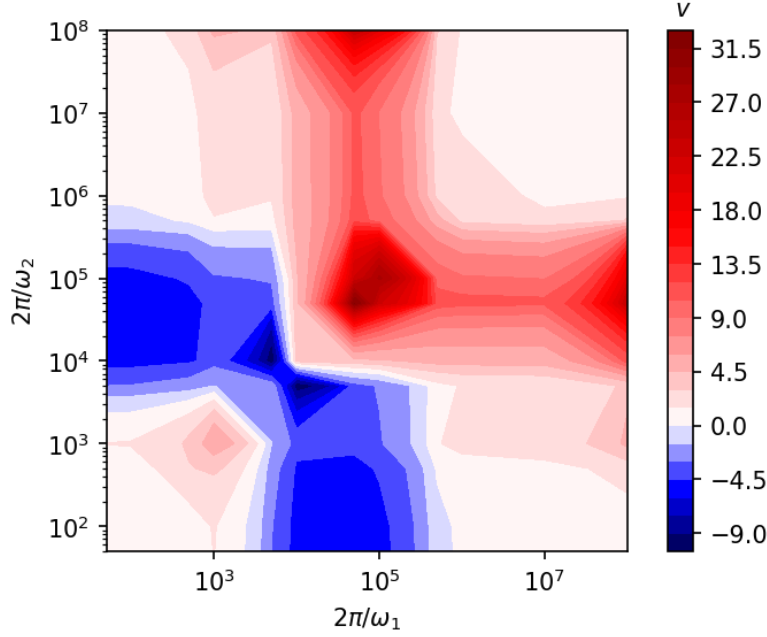


Figure 3. Heat map of the skyrmion velocity v in the negative x (blue) and positive x (red) directions for the system in Fig. 2 as a function of $2\pi/\omega_2$ versus $2\pi/\omega_1$. In some cases, multiple velocity reversals can occur as a function of changing frequency. Along the line $2\pi/\omega_1 = 2\pi/\omega_2$, the system can be regarded as being driven by a single ac frequency, yet there are still ratchet reversals in the velocity response.

above $2\pi/\omega_2 = 5 \times 10^4$. The overall magnitude of the motion is much larger than that shown in Fig. 2(a). For the sample with $2\pi/\omega_1 = 5 \times 10^4$ in Fig. 2(c), the velocity is weakly negative at low $2\pi/\omega_2$ and reverses to the positive x direction for $2\pi/\omega_2 > 1 \times 10^4$. The magnitude of the maximum positive velocity is nearly six times larger than the magnitude of the maximum negative velocity. In Fig. 2(d) at $2\pi/\omega_1 = 1 \times 10^6$, the motion is only in the positive x direction with a velocity peak near $2\pi/\omega_2 = 1 \times 10^5$. The results in Fig. 2 indicate that multiple reversals in the direction of motion can occur as the frequency of the ac drive is varied.

In Fig. 3 we construct a skyrmion velocity map as a function of $2\pi/\omega_2$ versus $2\pi/\omega_1$ for the system in Figs. 1 and 2, where regions of positive and negative direction motion appear along with regions in which no directed motion occurs. Multiple velocity reversals can occur depending on the manner in which the frequency is swept. The greatest velocity magnitude occurs for positive x direction motion when $2\pi/\omega_1 \approx 2\pi/\omega_2 = 1 \times 10^5$. When $2\pi/\omega_2 > 1 \times 10^6$, the motion is always in the positive x direction. Along the line $2\pi/\omega_1 = 2\pi/\omega_2$, the system can be considered as being driven by a single frequency, and even in this case, there are still multiple reversals from positive to negative velocity and back to positive velocity again.

We next consider the effects of applying a periodic pulse instead of a sinusoidal drive, which makes the transition from positive to negative motion easier to distinguish. To generate the periodic pulse, we set the E field along $\theta = 30^\circ$ during

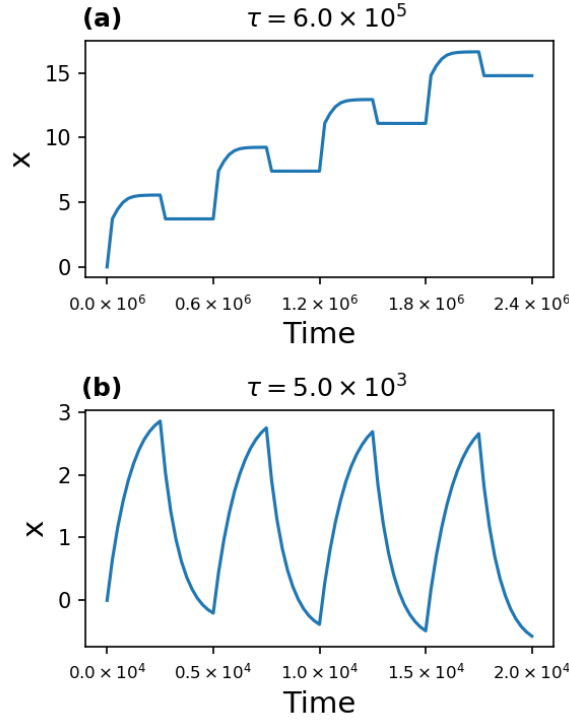


Figure 4. The time series of the center of mass motion of the skyrmion under a square pulse drive with period (a) $\tau = 6 \times 10^5$, where the net motion is in the positive x direction, and (b) $\tau = 5 \times 10^3$, where the net motion is in the negative x direction. The nature of the movement is different during the first portion of each pulse compared to the second part of each pulse.

the first half of each drive cycle, and then set it to $\theta = 0^\circ$ during the second half of each drive cycle. In this case we consider only a single driving frequency.

In Fig. 4 we plot the x position of the skyrmion center of mass as a function of time during four drive cycles in a sample where the periodic square pulse drive is applied with a period of $\tau = 6 \times 10^5$. The skyrmion moves easily along the positive x direction during the $\theta = 30^\circ$ portion of the drive cycle, with the most rapid motion occurring just after this field is first applied, while during the $\theta = 0^\circ$ portion of the drive cycle, the skyrmion moves briefly backwards before stalling and remaining stationary for the remainder of the drive cycle. In Fig. 4, when the square pulse drive period is reduced to $\tau = 5 \times 10^3$, the skyrmion has a slow net motion along the negative x direction. Here, there is a more rapid motion in the negative direction during the second half of the driving cycle compared to the more sluggish forward motion during the first half of the driving cycle.

In Fig. 5 we show a series of plots of the skyrmion center of mass x position versus time for varied square pulse frequencies from high to low. In Fig. 5(a), where the pulse period is $\tau = 5 \times 10^4$, there is strong motion in the forward direction. For $\tau = 2 \times 10^4$ in Fig. 5(b), no directed motion occurs. In Fig. 5(c) for $\tau = 1.4 \times 10^4$, there is a weak motion in the negative x direction, which becomes more prominent when $\tau = 8 \times 10^3$

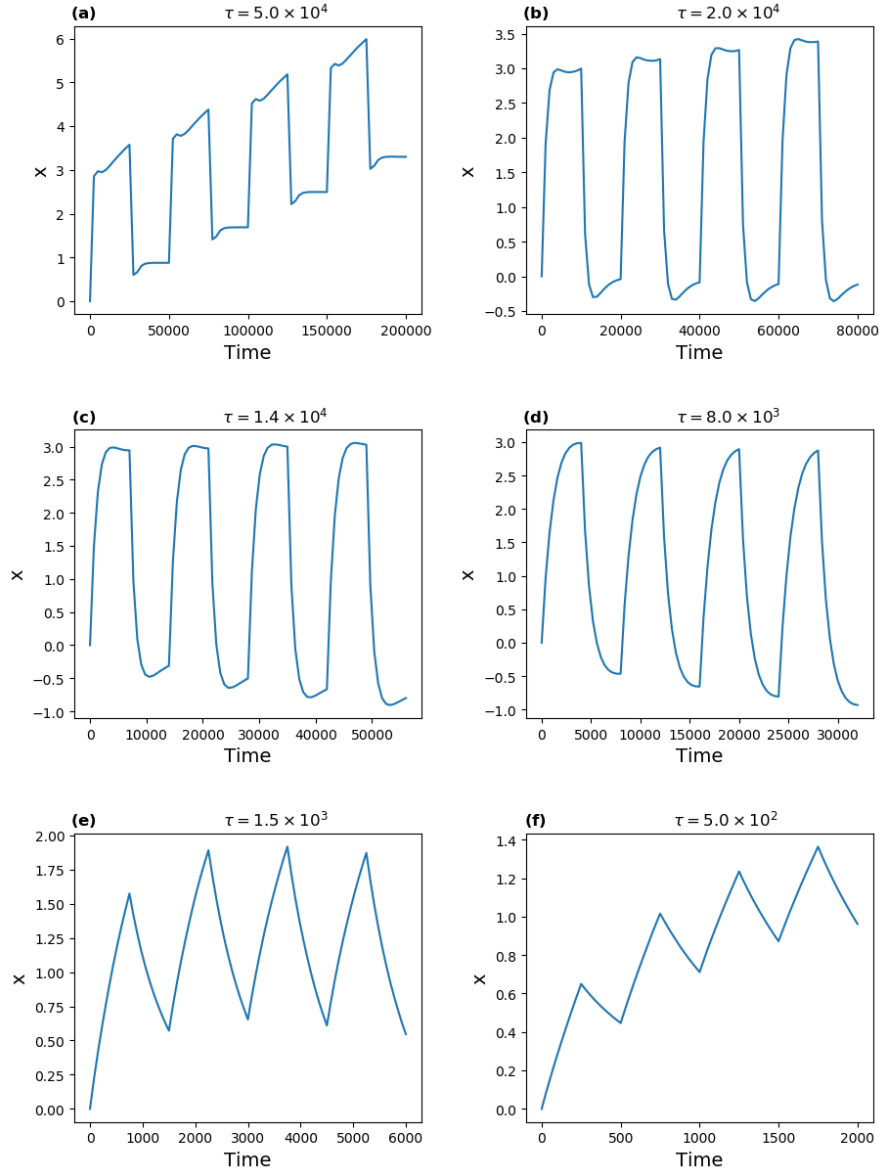


Figure 5. The time series of the skyrmion center of mass position x for a system with a single periodic pulse drive of period τ . (a) At $\tau = 5 \times 10^4$ there is strong forward motion. (b) At $\tau = 2 \times 10^4$, no directed motion occurs. (c) At $\tau = 1.4 \times 10^4$, the motion is in the negative x direction. (d) Similar negative x direction motion appears for $\tau = 8 \times 10^3$. (e) At $\tau = 1.5 \times 10^3$ there is no net motion. (f) At $\tau = 5 \times 10^2$, the motion is in the forward direction.

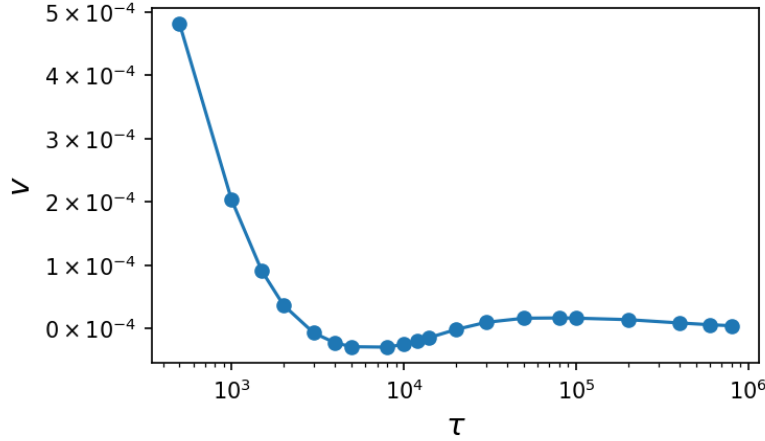


Figure 6. The skyrmion velocity v versus period τ for the system from Fig. 5 with a pulse drive shows a series of reversals from positive to negative directed motion.

as shown in Fig. 5(d). At $\tau = 1.5 \times 10^3$ in Fig. 5(e) there is no net motion, while for $\tau = 5 \times 10^2$, Fig. 5(f) indicates that forward motion appears. Here we find that a series of reversals in the velocity occur as a function of changing pulse frequency.

We plot the skyrmion velocity v versus the pulse drive period τ in Fig. 6, where we find a series of velocity reversals from positive motion for periods $\tau < 2 \times 10^3$, to negative motion, to a region of no motion, and finally to positive motion again. For the highest pulse periods, the skyrmion remains nearly static since the pulses become so rapid that the director field is no longer able to respond to the ac driving.

4. Discussion

Our results indicate that multiple reversals in the directed motion can occur for LC skyrmions under different ac drive conditions. The behavior is similar to the ratchet effect observed in particle-like systems with an ac drive when the particles are coupled to an asymmetric substrate [18]. In the ratchet systems, the particle moves along the easy direction of the asymmetric substrate; however, when multiple particles are present, collective interactions can induce reversals or even multiple reversals of the direction of ratchet motion [18, 27, 28, 29].

It is also possible for ratchet effects to occur in the absence of an asymmetric substrate when some other form of asymmetry comes into play, such as a nonlinear damping constant. This can happen when particles are coupled to other particles, as previously studied for superconducting vortices [30] or assemblies of colloidal particles [31], where the effective damping of each particle develops a velocity dependence or a frequency dependence. For example, if the ac drive is itself asymmetric, with a fast portion spanning a short time t_1 with a large force F_1 and a slow portion spanning a longer time t_2 with a smaller force F_2 , such that $F_1 t_1 = -F_2 t_2$, there is no net applied force during each driving period of $T = t_1 + t_2$. A single particle with a fixed damping constant η traverses a distance $d_1 = (1/\eta)F_1 t_1$ during the first portion of the

drive cycle and a distance $d_2 = (1/\eta)F_2t_2$ in the opposite direction during the second portion of the drive cycle. If η has no dependence on the drive, then $d_1 = d_2$ and there is no net ratcheting motion of the particle. If, on the other hand, η exhibits some nonlinear time dependence, such that for high drive F there is a shear thinning effect, then $d_1 > d_2$ and the particle will move in the positive direction. If instead there is shear thickening, then $d_2 > d_1$ and net motion will occur in the negative direction. Effects of this type have been observed in a system where each particle has a fixed damping coefficient but the collective effects between particles in the surrounding medium produce an effective nonlinear velocity dependence of the drag, leading to the emergence of a ratchet effect [31].

For the LC skyrmion system we consider here, there is only a single skyrmion present, but because the model is in the continuum limit, collective modes can arise among the degrees of freedom. Our results for the pulse drive suggest that the net forward or backward motion originates from a nonlinear drag effect that is produced by asymmetric ac oscillations in the skyrmion shape. Beyond LC skyrmions, the effects we observe could also be relevant for skyrmions in magnetic systems or for soft matter systems containing bubble like shapes such as vesicles undergoing some sort of asymmetric periodic shape change or expansion [32]. It would also be interesting to couple this motion to some kind of substrate in order to generate controlled directed motion.

5. Summary

We have shown that liquid crystal skyrmions under an ac electric field drive biased along the positive y direction with either multiple or single frequencies can show directed motion in both the forward and backward directions along the x axis as a function of frequency. We map the dynamic regime diagram for this motion, showing that there are optimal frequencies for motion and that multiple direction reversals can occur even when only a single frequency is present. We have also considered pulsed drives with a single frequency and found that multiple reversal effects can occur. The ability to direct and precisely steer the motion of these deformable particles suggests that this could be an interesting future route to the construction of soft robotic skyrmion systems.

Acknowledgments

This work was supported by the US Department of Energy through the Los Alamos National Laboratory. Los Alamos National Laboratory is operated by Triad National Security, LLC, for the National Nuclear Security Administration of the U. S. Department of Energy (Contract No. 892333218NCA000001).

References

- [1] Rößler U K, Bogdanov A N and Pfleiderer C 2006 *Nature (London)* **442** 797–801
- [2] Mühlbauer S, Binz B, Jonietz F, Pfleiderer C, Rosch A, Neubauer A, Georgii R and Böni P 2009 *Science* **323** 915–919
- [3] Yu X Z, Onose Y, Kanazawa N, Park J H, Han J H, Matsui Y, Nagaosa N and Tokura Y 2010 *Nature (London)* **465** 901–904
- [4] Nagaosa N and Tokura Y 2013 *Nature Nanotechnol.* **8** 899–911
- [5] Fukuda J and Žumer S 2011 *Nature Commun.* **2** 246

- [6] Ackerman P J, Trivedi R P, Senyuk B, van de Lagemaat J and Smalyukh I I 2014 *Phys. Rev. E* **90**(1) 012505
- [7] Leonov A O, Dragunov I E, Rößler U K and Bogdanov A N 2014 *Phys. Rev. E* **90**(4) 042502
- [8] Nych A, Fukuda J, Ognysta U, Žumer S and Mušević I 2017 *Nature Phys.* **13** 1215
- [9] Ackerman P J, Boyle T and Smalyukh I I 2017 *Nature Commun.* **8** 673
- [10] Duzgun A, Selinger J V and Saxena A 2018 *Phys. Rev. E* **97**(6) 062706
- [11] Sohn H R O, Liu C D and Smalyukh I I 2019 *Nature Commun.* **10** 4744
- [12] Long C and Selinger J V 2021 *arXiv:2109.07314*
- [13] Moon K W, Kim D H, Je S G, Chun B S, Kim W, Qiu Z Q, Choe S B and Hwang C 2016 *Sci. Rep.* **6** 20360
- [14] Wang W, Beg M, Zhang B, Kuch W and Fangohr H 2015 *Phys. Rev. B* **92**(2) 020403
- [15] Yuan H Y, Wang X S, Yung M H and Wang X R 2019 *Phys. Rev. B* **99**(1) 014428
- [16] Chen W, Liu L, Ji Y and Zheng Y 2019 *Phys. Rev. B* **99**(6) 064431
- [17] Chen W, Liu L and Zheng Y 2020 *Phys. Rev. Applied* **14**(6) 064014
- [18] Reimann P 2002 *Phys. Rep.* **361** 57–265
- [19] Reichhardt C, Ray D and Reichhardt C J O 2015 *New J. Phys.* **17** 073034
- [20] Ma X, Reichhardt C J O and Reichhardt C 2017 *Phys. Rev. B* **95**(10) 104401
- [21] Migita K, Yamada K and Nakatani Y 2020 *Appl. Phys. Express* **13** 073003
- [22] Göbel B and Mertig I 2021 *Sci. Rep.* **11** 3020
- [23] Souza J C B, Vizarrim N P, Reichhardt C J O, Reichhardt C and Venegas P A 2021 *Phys. Rev. B* **104**(5) 054434
- [24] Duzgun A, Nisoli C, Reichhardt C J O and Reichhardt C 2020 *Soft Matter* **16** 3338–3343
- [25] Duzgun A and Nisoli C 2021 *Phys. Rev. Lett.* **126**(4) 047801
- [26] Tai J S B and Smalyukh I I 2020 *Phys. Rev. E* **101**(4) 042702
- [27] de Souza Silva C C, de Vondel J V, Morelle M and Moshchalkov V V 2006 *Nature (London)* **440** 651–654
- [28] Lu Q, Reichhardt C J O and Reichhardt C 2007 *Phys. Rev. B* **75**(5) 054502
- [29] McDermott D, Olson Reichhardt C J and Reichhardt C 2016 *Soft Matter* **12**(41) 8606–8615
- [30] Cole D, Bending S, Savel'ev S, Grigorenko A, Tamegai T and Nori F 2006 *Nature Mater.* **5** 305–311
- [31] Reichhardt C, Reichhardt C J O and Hastings M B 2005 *Phys. Lett. A* **342** 162–167
- [32] Metselaer L, Doostmohammadi A and Yeomans J M 2019 *J. Chem. Phys.* **150** 064909